Radiative transfer

ENV-409

Characteristics of light and radiation

As electromagnetic wave
- amplitude
- frequency
- (polarization)

As radiometric quantities
- intensity
- flux
- power

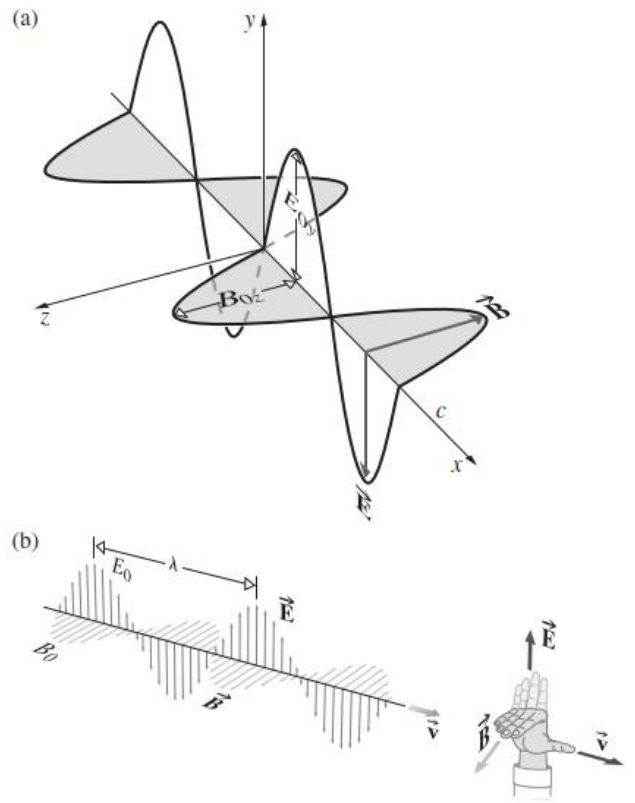

Figure 3.14 (*a*) Orthogonal harmonic $\vec{E}$- and $\vec{B}$-fields for a plane polarized wave. (*b*) The wave propagates in the direction of $\vec{E} \times \vec{B}$.

Hecht, 2017

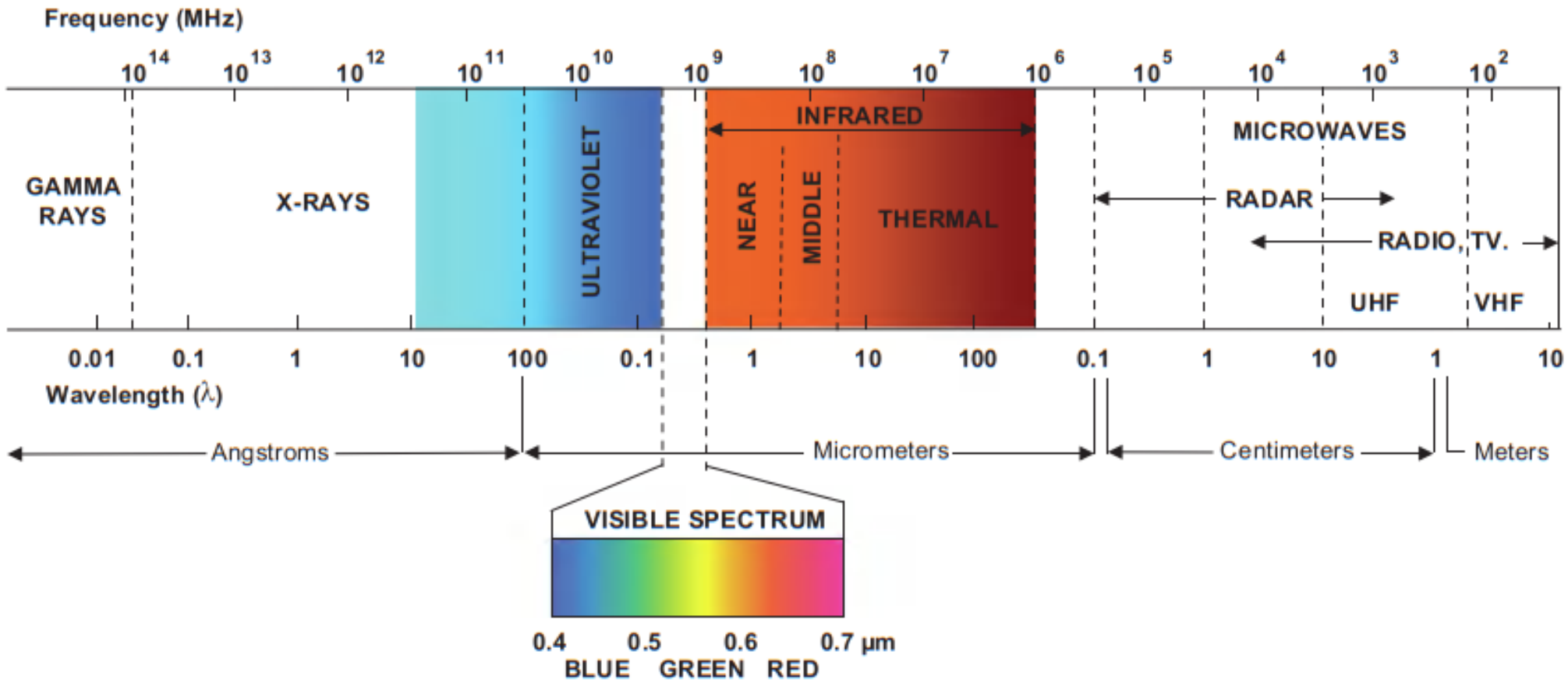

Chuvieco, 2020

Properties of matter

Bulk matter

- polarization density (volumetric concentration of electric dipoles)
- complex relative permittivity / dielectric function
- complex refractive index

Atoms and molecules

- polarizability

Light-matter interactions

Conceptual model 1:
Bohr's model of the atom

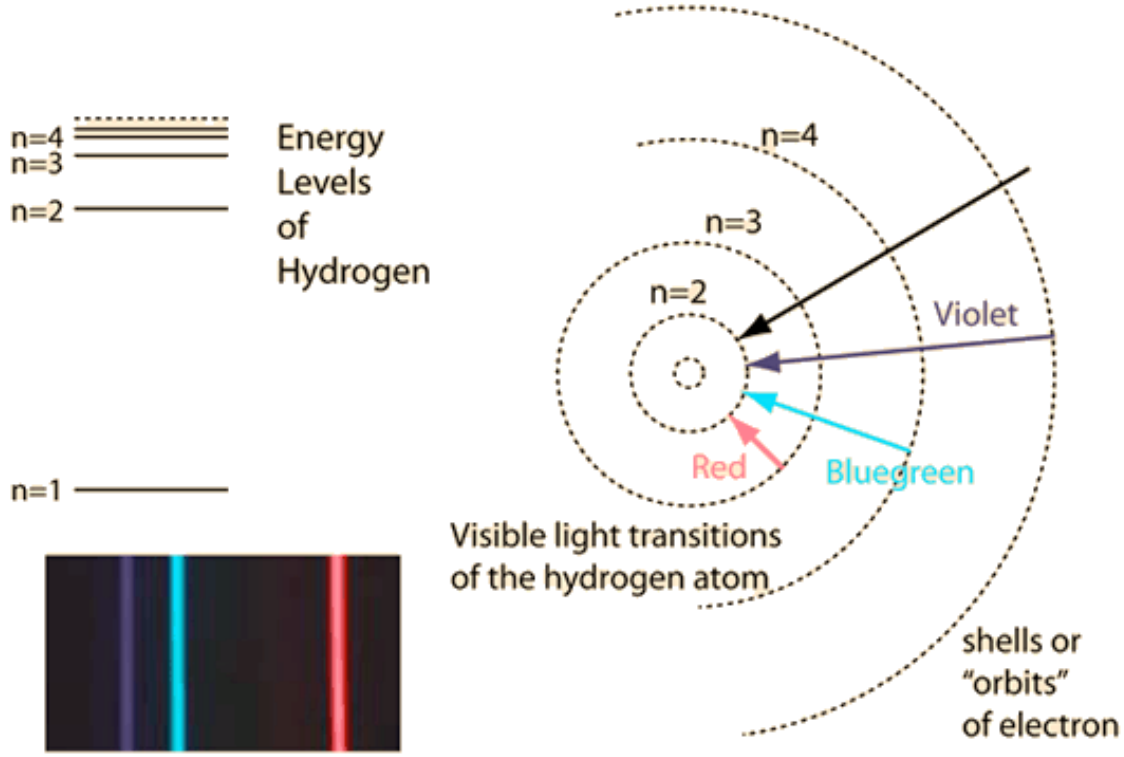

Hyperphysics, Georgia State Univ.

Ultraviolet radiation

- electronic transitions (non-ionizing) induce excited states
- Ionizing at higher energies (*sunburn and skin cancer*)

Visible radiation

- electronic transitions induce excited states

Conceptual model 2:
(an)harmonic oscillators

Infrared radiation induces changes in vibrational and rotational motion

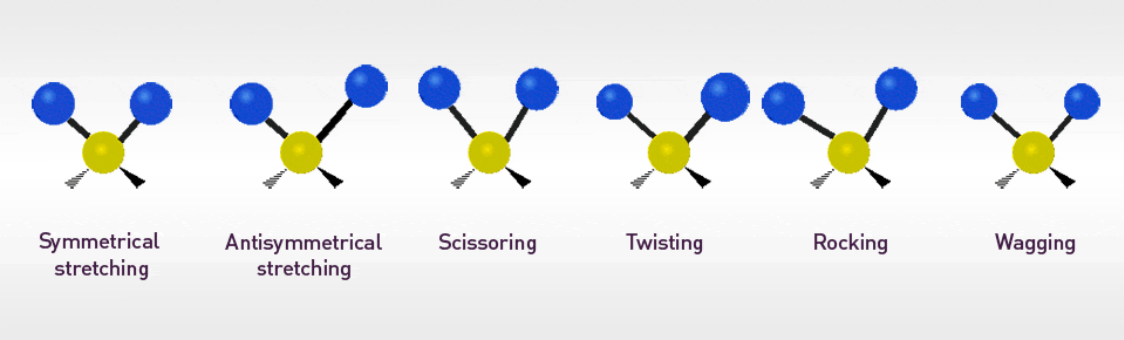

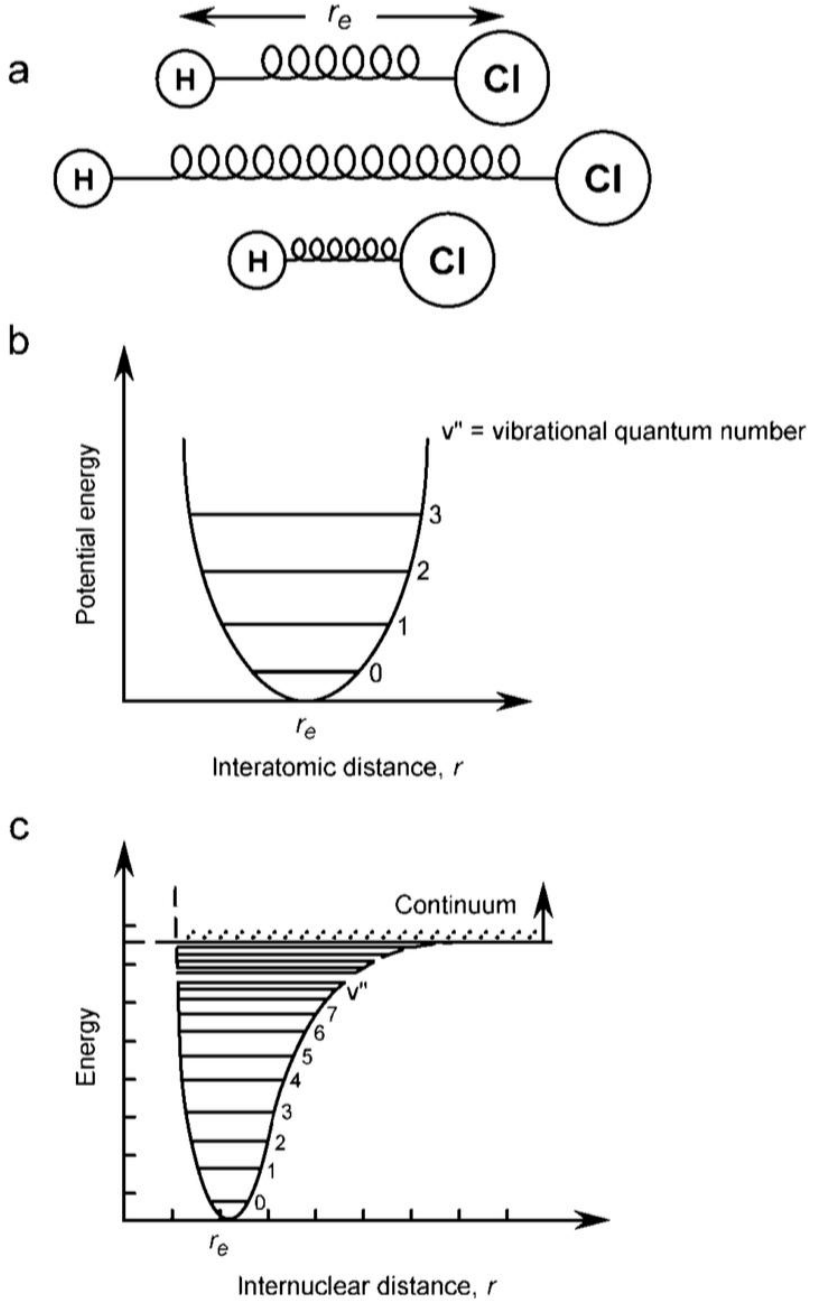

FIGURE 3.2 (a) Vibration of diatomic molecule, HCl, (b) potential energy of an ideal harmonic oscillator, and (c) an anharmonic oscillator described by the Morse function.

Finlayson-Pitts and Pitts, 1999
https://www.analyticon.eu/en/nir.html

Polarizability

Tendency of atom or molecule to be polarized by an external electric field

- *Orientational*: molecular alignment
- *Electronic*: distortion of electron cloud
- *Vibrational*: nuclear movement changes electronic charge distribution
- *Rotational*: rotational movement
- *Ionic*: ions in crystals

Results in a change in dipole moment

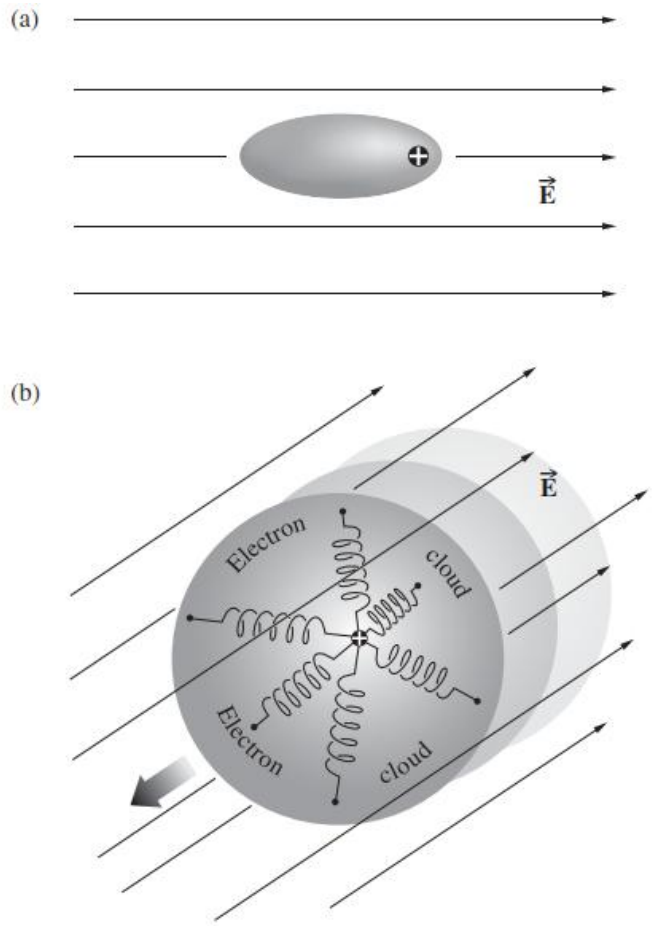

Figure 3.38 (*a*) Distortion of the electron cloud in response to an applied $\vec{E}$-field. (*b*) The mechanical oscillator model for an isotropic medium—all the springs are the same, and the oscillator can vibrate equally in all directions.

Hecht, 2017

Polarization density

- Number density of dipoles
- As external field separates positive and negative charges, electric field is changed
- *P* measures change in electric field due to medium

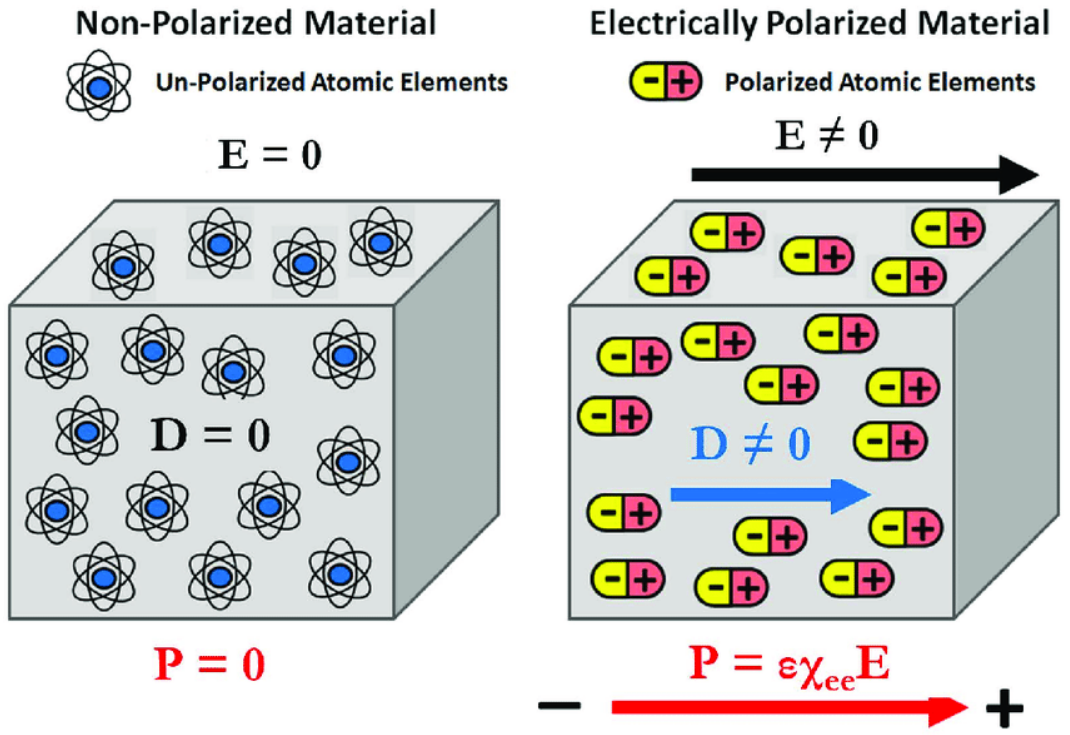

Danufane, 2021

Relating polarizability and polarization density

Changes to polarization density and dipole moment in response to external electric field.

$$\chi_e = \tilde{\epsilon}_r - 1$$
$$\sum_i N_i \boldsymbol{p}_i = \boldsymbol{P} = \epsilon_0 \chi_e \boldsymbol{E}$$
$$\boldsymbol{p}_i = \tilde{\alpha}_{\mathrm{pol},i} \boldsymbol{E}_{\mathrm{loc}}$$

Common models for relationship between incident and local electric field.

$$\boldsymbol{E}_{\mathrm{loc}} = \boldsymbol{E}$$
$$\boldsymbol{E}_{\mathrm{loc}} = \boldsymbol{E} + \frac{\boldsymbol{P}}{3\epsilon_0}$$

Leads to a relationship between atomic or molecular polarizability and permittivity. E.g., in the former case,

$$\tilde{\epsilon}_r = 1 + \frac{1}{\epsilon_0} \sum_i N_i \alpha_{\mathrm{pol},i}$$

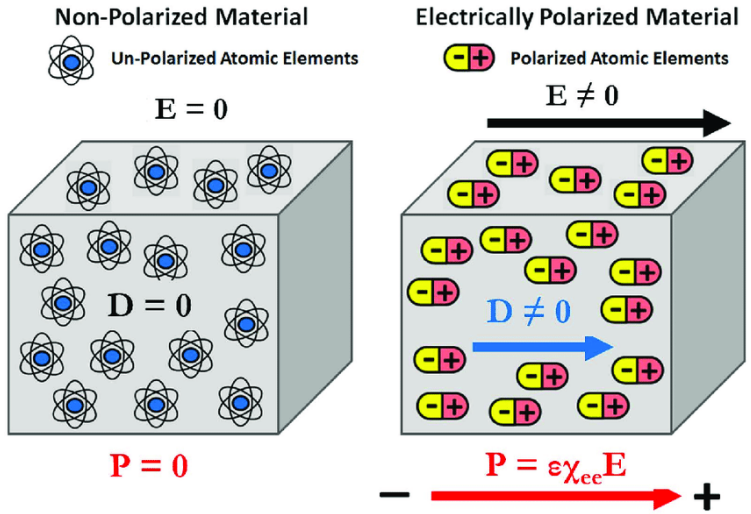

Danufane, 2021

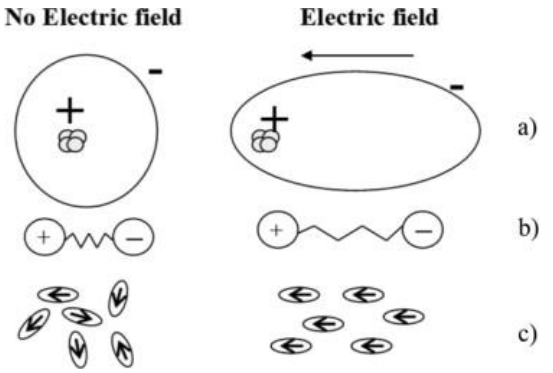

Posseme and Darnon, 2015

Classical damped (driven) harmonic oscillator

single oscillator for electron displacement

$$F = q_e E = m(\ddot{x} + \gamma\dot{x} + \omega_0^2 x)$$

solution gives displacement

$$x = \frac{q_e/m}{-\omega^2 + i\gamma\omega + \omega_0^2} E$$

from definition of dipole

$$\boldsymbol{p} = \frac{q_e^2/m}{-\omega^2 + i\gamma\omega + \omega_0^2} \boldsymbol{E}$$

atomic polarizability

$$\alpha = \frac{q_e^2/m\epsilon_0}{-\omega^2 + i\gamma\omega + \omega_0^2}$$

$$\omega_0 = \sqrt{\frac{k}{m}}$$

dipole moment

$\boldsymbol{p} = q\boldsymbol{r}$ or $p = qx$

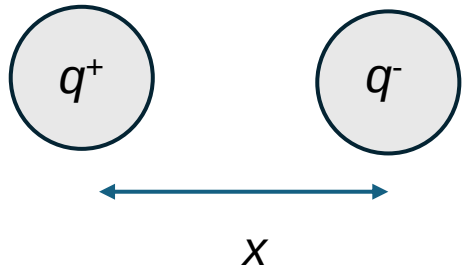

Model as

- ball attached to wall by spring (electronic)
- two balls attached by spring (vibrational)

From Feynman Lectures Vol. II Ch. 32

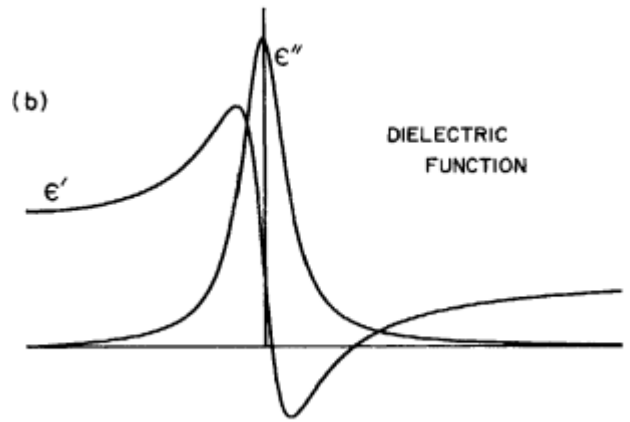

Figure 9.2 Characteristics of the one-oscillator (Lorentz) model.

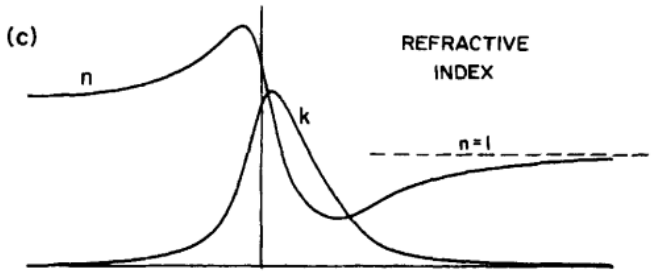

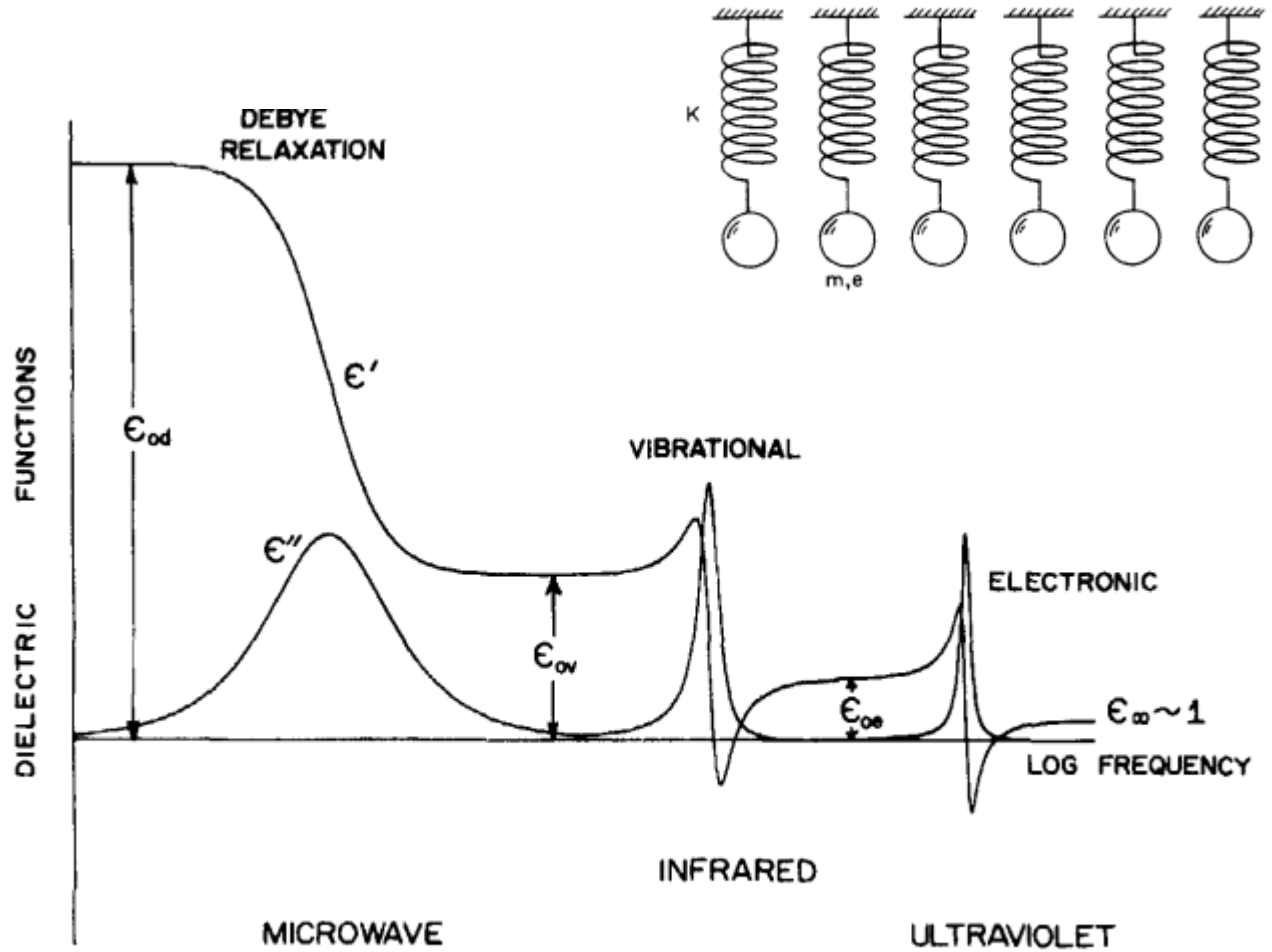

Figure 9.16 Schematic diagram of the frequency variation of the dielectric function of an ideal nonconductor.

Bohren and Huffman, 1983

Propagation of electric field in homogeneous medium

Maxwell's equation in isotropic, homogeneous medium (wave equation)

$$\nabla^2 \boldsymbol{E} - \frac{\tilde{\epsilon}_r}{c_0^2} \frac{\partial^2}{\partial t^2} \boldsymbol{E} = 0$$

Change from defining the medium in terms of complex dielectric function to complex refractive index.

$$\begin{aligned} \mathrm{Re}\left\{\tilde{\epsilon}_r\right\} &= n^2 - \kappa^2 \\ \mathrm{Im}\left\{\tilde{\epsilon}_r\right\} &= 2n\kappa \end{aligned}$$

Define *complex wave vector* via real and imaginary refractive indices.

$$\boldsymbol{k} = \frac{\omega}{c_0}(n + i\kappa)\hat{\boldsymbol{s}}$$

Solution to wave equation.

$$\boldsymbol{E} = \boldsymbol{E}_0 e^{i(\boldsymbol{k}\cdot\boldsymbol{r} - \omega t)}$$

Dispersion and attenuation

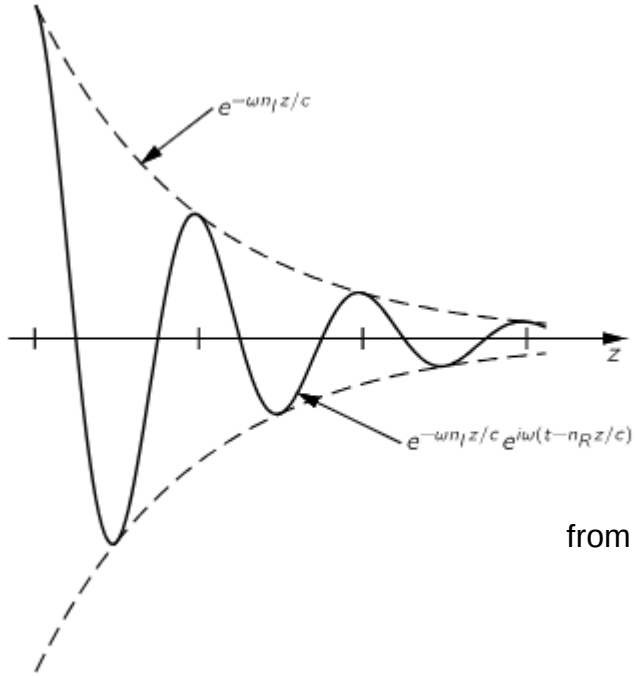

from Feyman lectures

Fig. 32–1. A graph of E_x for some instant t, if $n_I \approx n_R/2\pi$.

$$E = E_0 e^{-\omega z \kappa / c_0} e^{i\omega(t - z\, n/c_0)}$$

Hecht, 2017

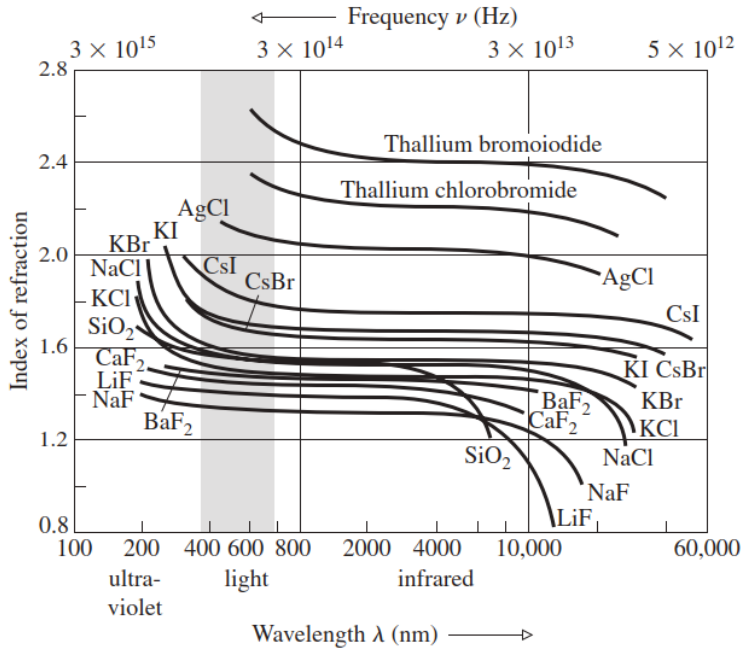

Figure 3.42 Index of refraction versus wavelength and frequency for several important optical crystals. (SOURCE: Data published by The Harshaw Chemical Co.)

Seinfeld and Pandis, 2006

TABLE 15.2 Refractive Indices of Atmospheric Substances at λ = 589 nm (Unless Otherwise Indicated)

	$m = n + ik$		
Substance	n	k	
Water	1.333	0 (see Table 15.1)	
Water (ice)	1.309		
NaCl	1.544	0	
H_2SO_4	1.426[a]	0	
NH_4HSO_4	1.473[b]	0	
$(NH_4)_2SO_4$	1.521[b]	0	
SiO_2	1.55	0	($\lambda = 550$ nm)
Carbon[c]	1.95	−0.79	($\lambda = 550$ nm)
Mineral dust[d]	1.56	−0.006	($\lambda = 550$ nm)

[a] Stelson (1990), assuming a 97% pure (by mass) mixture of H_2SO_4 with H_2O.
[b] Weast (1987).
[c] Bond and Bergstrom (2006) report a narrow range of refractive indices of light-absorbing carbon. The value in the table represents the upper limit.
[d] Tegen et al. (1996).

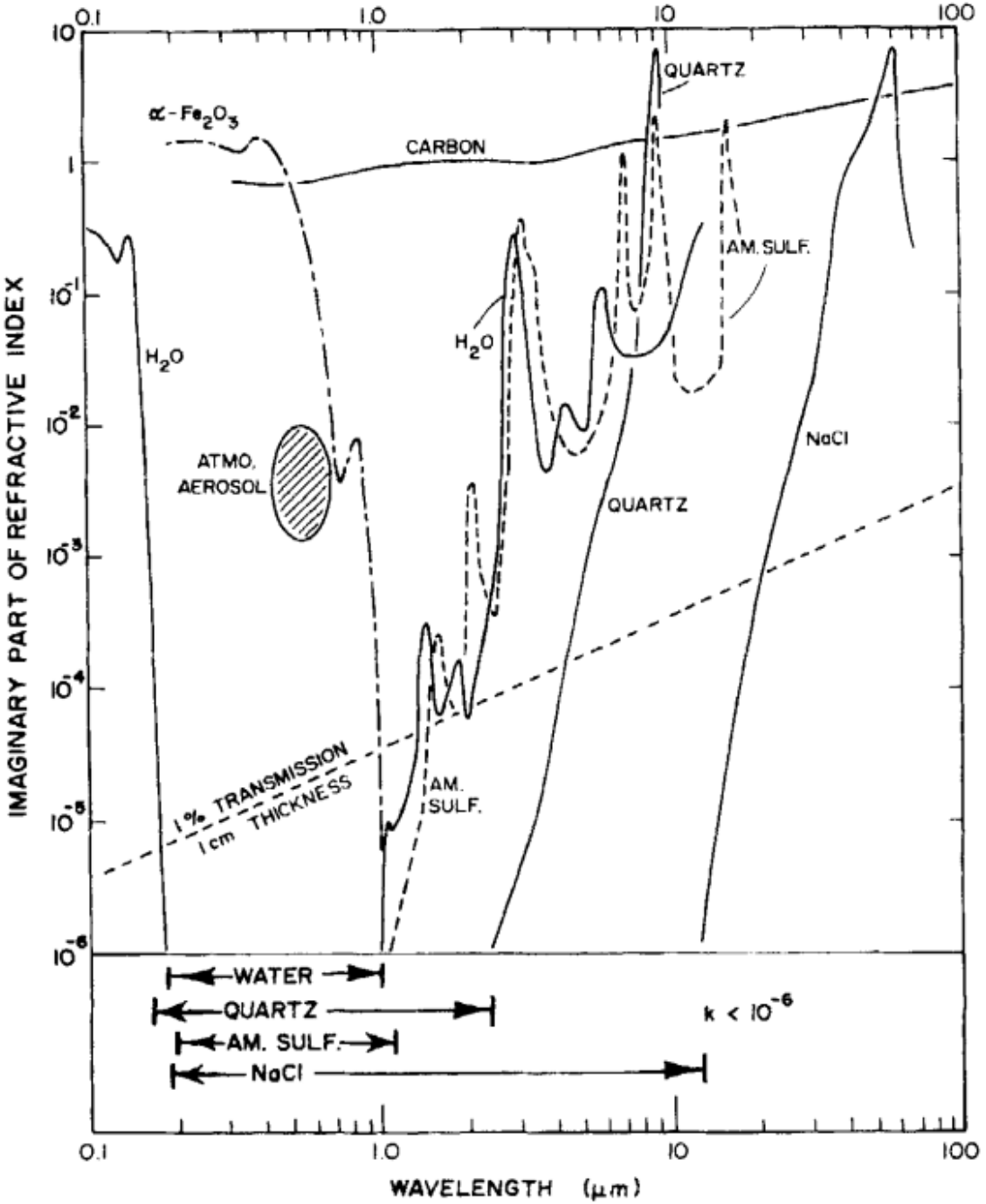

Figure 14.1 Imaginary part of the refractive index of several solids and liquids that are found as atmospheric particles.

Bohren and Huffman, 1983

Behavior at dielectric boundaries

planar / curved surfaces

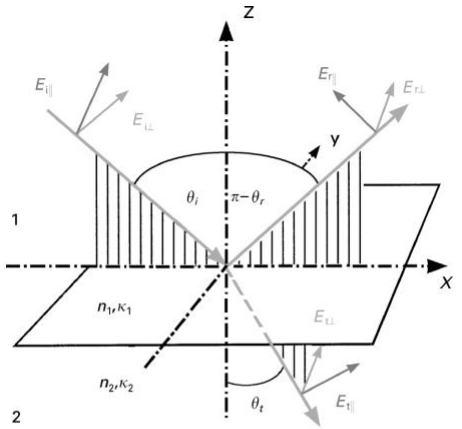

Figure 1 Specular reflection and transmission. The angles of incidence (i), reflection (r) and refraction (t) are denoted by θ_i, θ_r and θ_t, respectively. The corresponding electric field components are denoted by E. They are split into orthogonal portions, one parallel to the plane of incidence (x, z-plane) and the other perpendicular to this plane (parallel to y-axis). Accordingly, electric fields are referred to as parallel (||) and perpendicular ($\perp$) polarized; n_1, n_2, κ_1 and κ_2 denote the refractive and absorption indices in the two media.

Fringeli, 2017

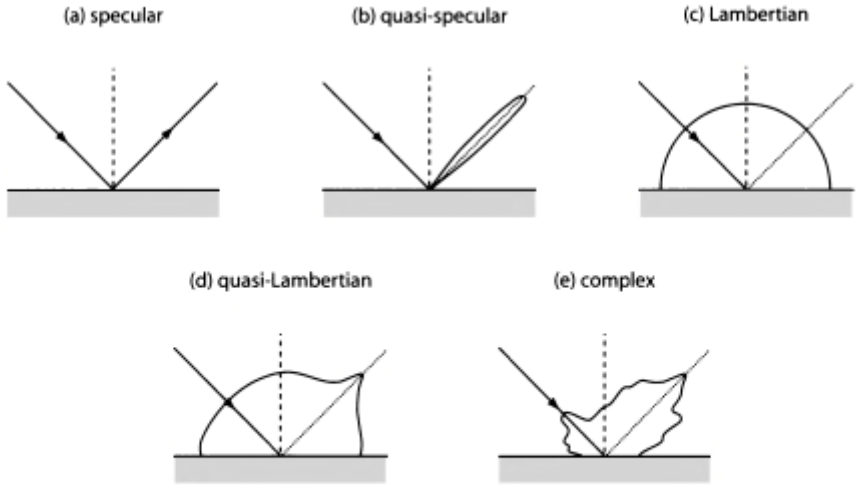

Fig. 5.3: Examples of various types of surface reflection, presented in the form of polar plots in which the distance of the curve to the reflection point on the surface represents the relative intensity of reflected radiation in that direction.

Petty, 2006

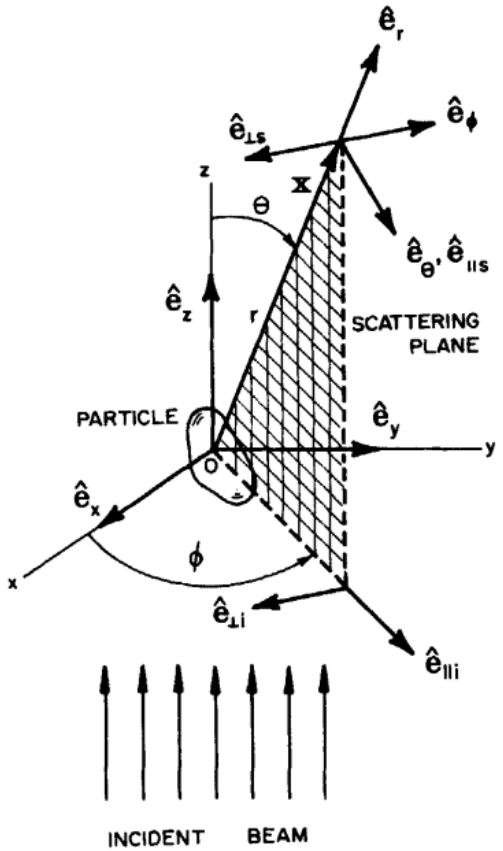

Figure 3.3 Scattering by an arbitrary particle.

Bohren and Huffman, 1983

From near-field to far-field

- Over small distances (relative to wavelength), coherent interactions among EM waves are important – sum wave amplitudes

- Over greater distances, incoherent interactions – sum intensities (radiance / irradiance)

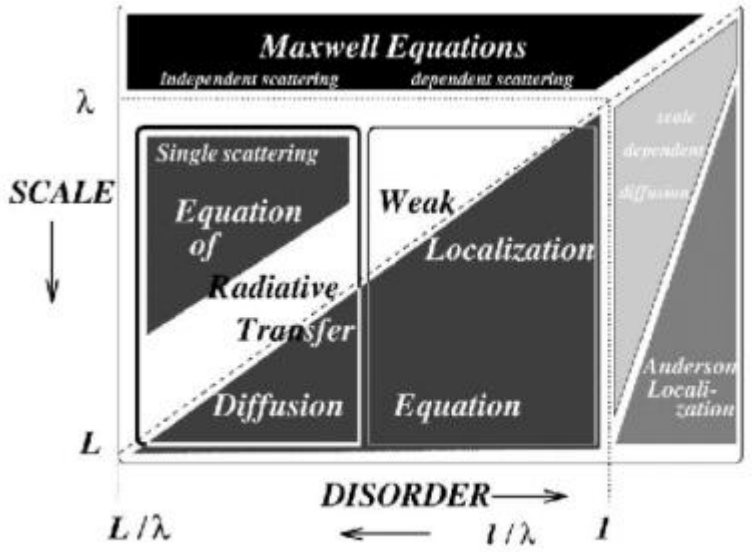

van Tiggelen and H. Stark, *Rev. Mod. Phys.*, 2000

Radiometric quantities

$$\Phi \qquad \text{Power}$$

$$I = \frac{\partial^2 \Phi}{\partial A \partial \Omega} \qquad \text{Radiance}$$

$$J(\boldsymbol{r}, \Omega_0) = \frac{\partial \Phi}{\partial A} = \lim_{\Delta\Omega \to 0} I(\boldsymbol{r}, \Omega) \Delta\Omega = \frac{n c_0 \epsilon_0}{2} |\boldsymbol{E}(\boldsymbol{r})|^2 \quad \text{Irradiance}$$

Table 2.1 SI radiometry units.

Quantity	SI unit (abbr.)	Notes
Radiant energy	J	Energy
Radiant flux	W	Also called radiant power
Radiant intensity	W sr^{-1}	Power per unit solid angle
Radiance	W sr^{-1} m^{-2}	Power per unit solid angle per unit area
Irradiance	W m^{-2}	Power incident on a surface
Radiant exitance or Radiant emitance	W m^{-2}	Power emitted from a surface
Radiosity	W m^{-2}	Emitted + reflected power from a surface
Spectral radiance	W sr^{-1} m^{-3} or W sr^{-1} m^{-2} Hz^{-1}	
Spectral irradiance	W m^{-3} or W m^{-2} Hz^{-1}	

Table adapted from [1].

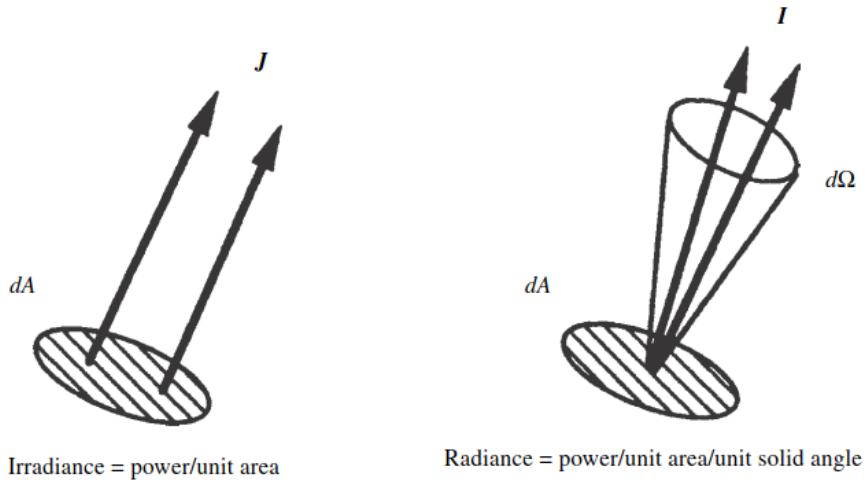

Figure 5.1 Irradiance and radiance.

Hapke, 2012

Seager, 2010

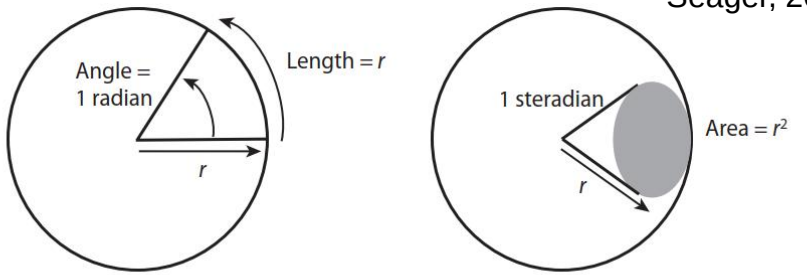

Figure 2.2 Definition of a radian (left panel) and a steradian (right panel). A steradian is related to the surface area of a sphere as a radian is related to the circumference of a circle. In 2D 1 radian is the angle subtended at the center of a circle by an arc length equal to the radius of a circle. In 3D 1 steradian is a measure of solid angle and is the solid angle subtended at the center of a sphere of radius r having an area r^2.

$$d\Omega = \sin\theta d\theta d\phi$$

Equation of Radiative Transfer and Beer-Lambert-Bouguer (BLB) Law

Basic equation

$$dI(\boldsymbol{r},\nu) = -I(\boldsymbol{r},\nu)\, d\tau(\nu) + dS$$
$$d\tau = \sum_i N_i \sigma_i ds$$

sources: multiple scattering, emission

Removal of radiation by absorption and scattering

$$\sigma = \sigma_{\mathrm{ext}} = \sigma_{\mathrm{abs}} + \sigma_{\mathrm{sca}}$$

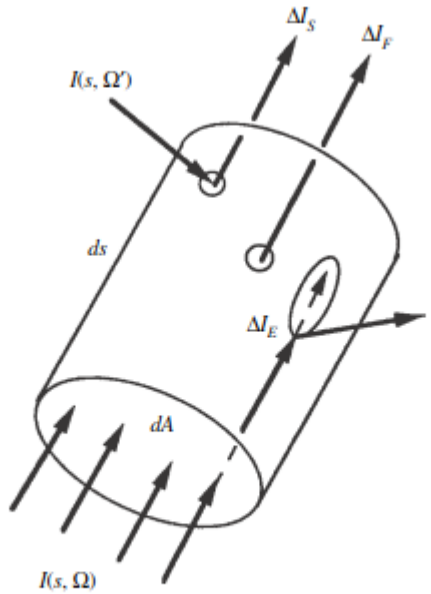

Figure 7.3 Schematic diagram of the changes in the radiance as it traverses the cylindrical volume *dsdA*.

Optical depth integrated over path length *l* (BLB assumption)

Hapke, 2012

$$\tau = \ell \left(\sum_{i \in \mathrm{gases}} N_i \sigma_{\mathrm{ext},i} + \sum_{i \in \mathrm{particles}} N_i \sigma_{\mathrm{ext},i} + \sum_{i \in \mathrm{hydrometeors}} N_i \sigma_{\mathrm{ext},i} \right)$$

Account for surface reflection

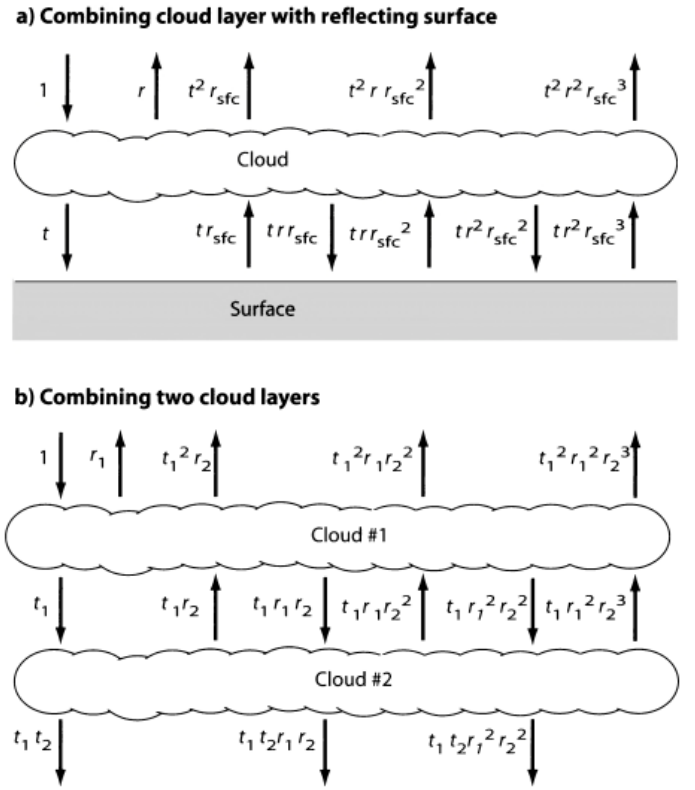

Fig. 13.10: Depiction of the first few transmittance and reflectance contributions when multiple reflections occur between (a) a cloud layer and a non-black surface, and (b) two cloud layers.

Petty, 2006

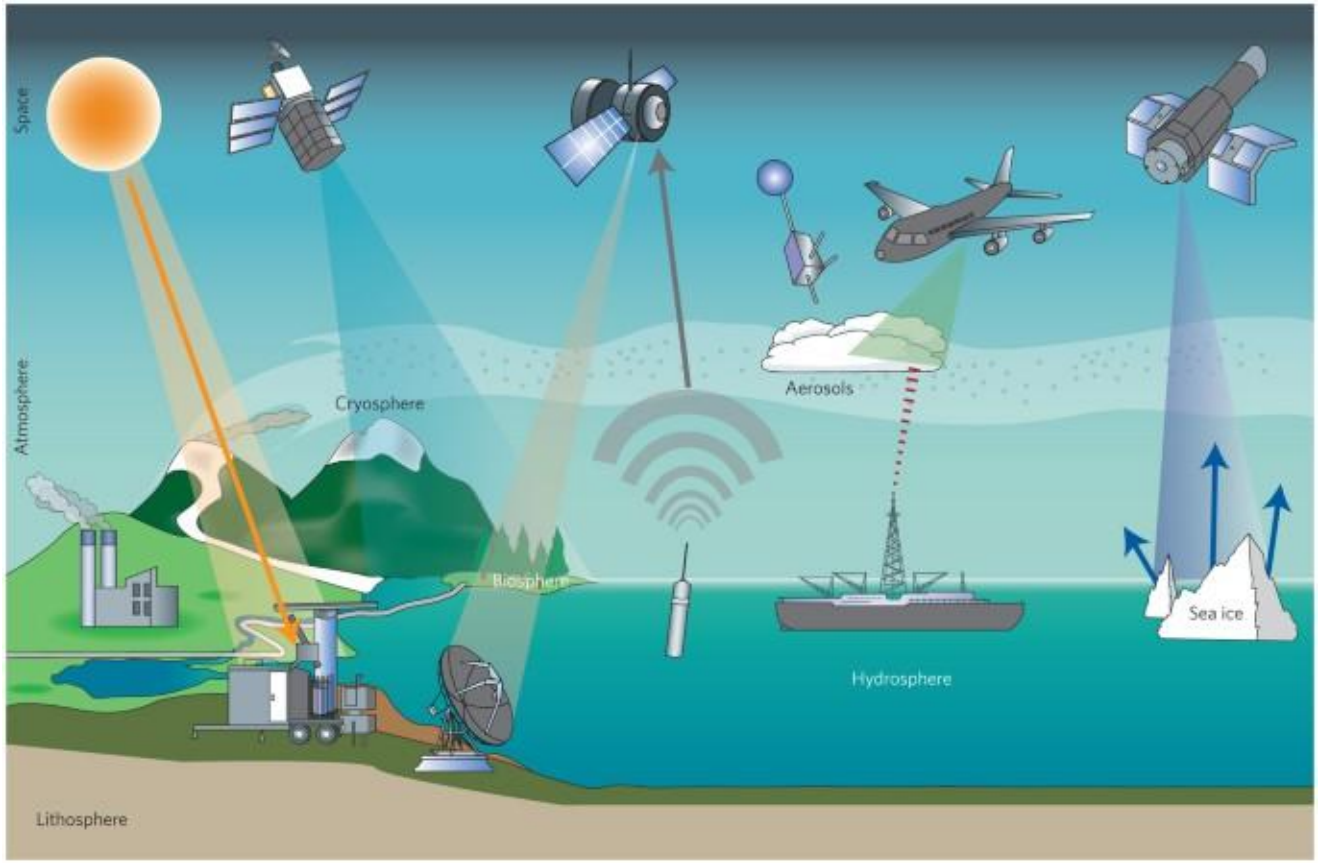

Yang et al., 2013

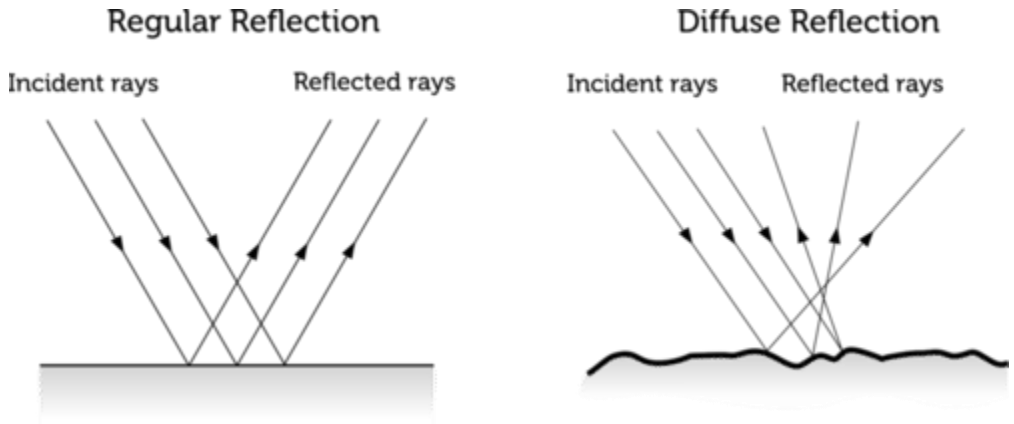

ck12.org

Two-stream RTE for plane-parallel cloud layers
and boundary conditions at top of atmosphere and surface

Model uses

Predict radiative forcing due to changes in atmospheric composition due to emissions

Inverse model atmospheric concentrations or surface properties

Simulate atmospheric radiation to estimate the spectral irradiance at a give position (e.g., for photochemical calculations)

Modes of measurement

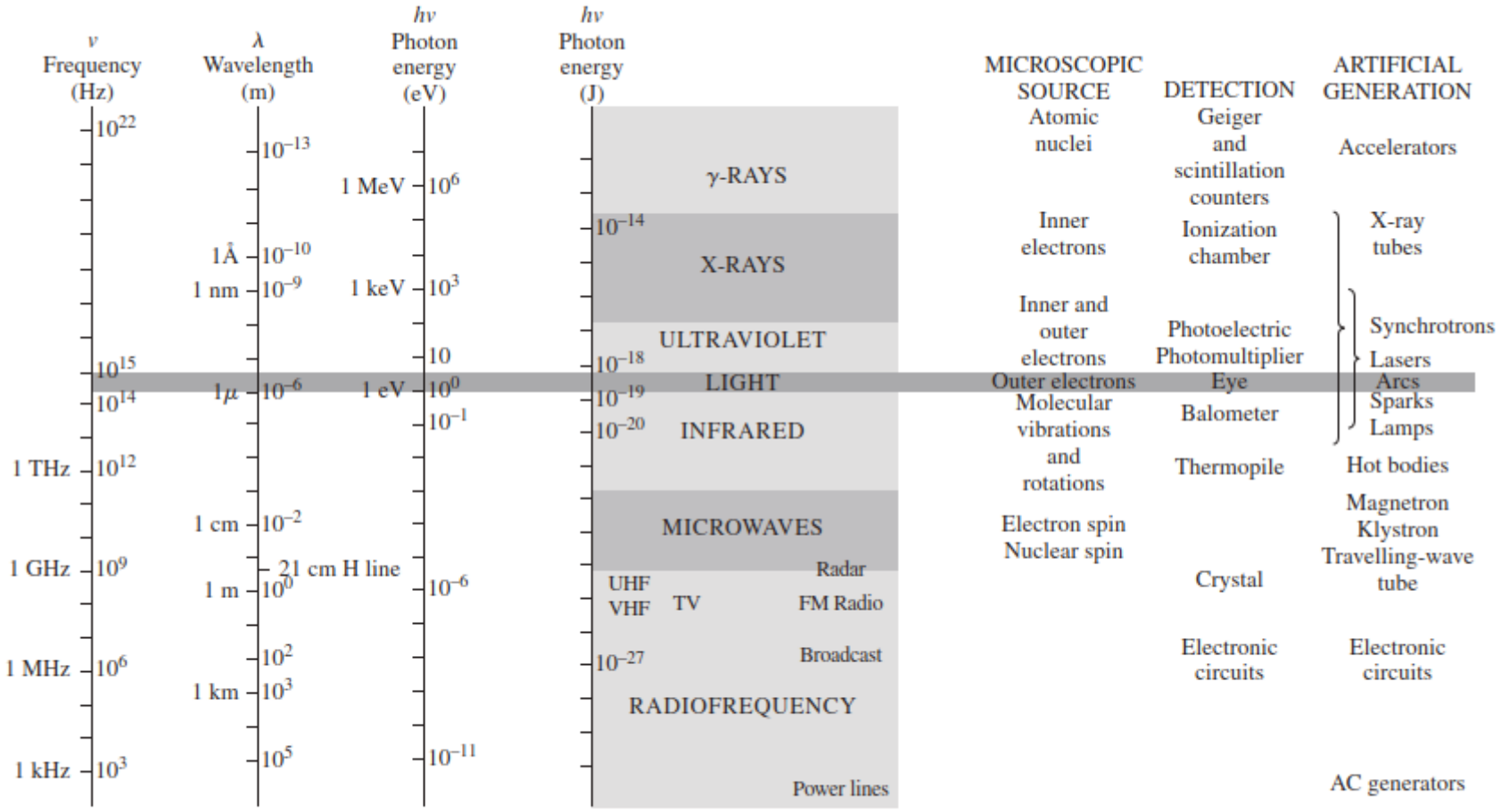

Figure 3.43 The electromagnetic-photon spectrum.

Hecht, 2017

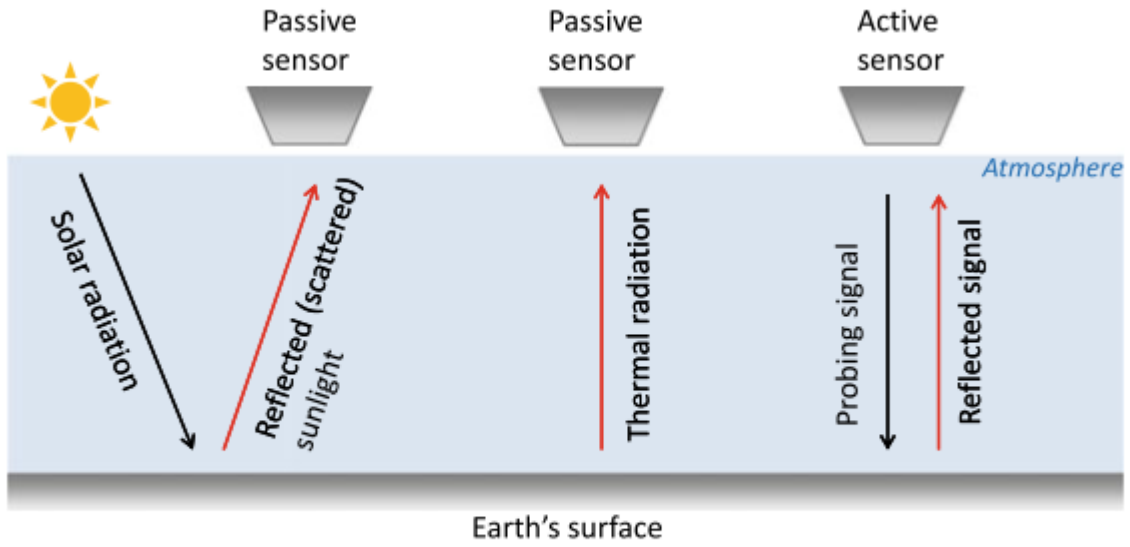

Fig. 1.1 Three schemes of remote sensing approach. Left and middle pictures refer to the passive remote sensing, while the right scheme shows the active remote sensing setup

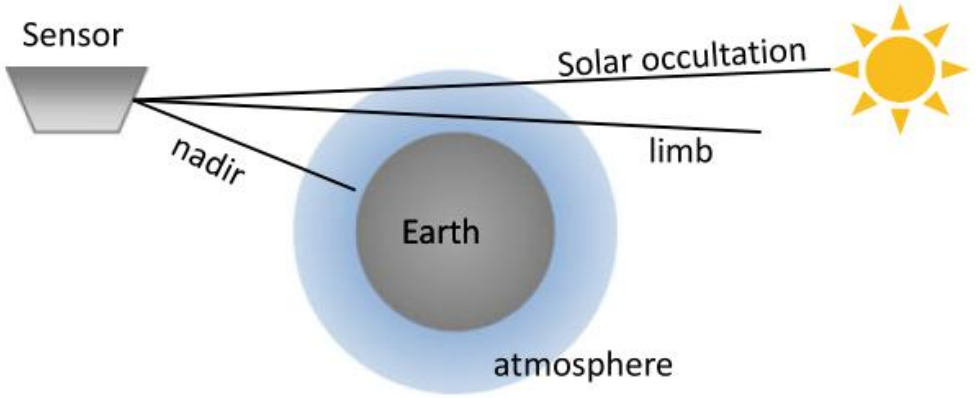

Fig. 1.5 Nadir, limb and solar measurement modes

Efremenko and Kokhanovsky, 2021

Lidar

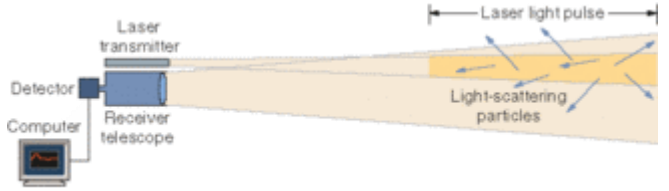

Laser Focus World

Radar

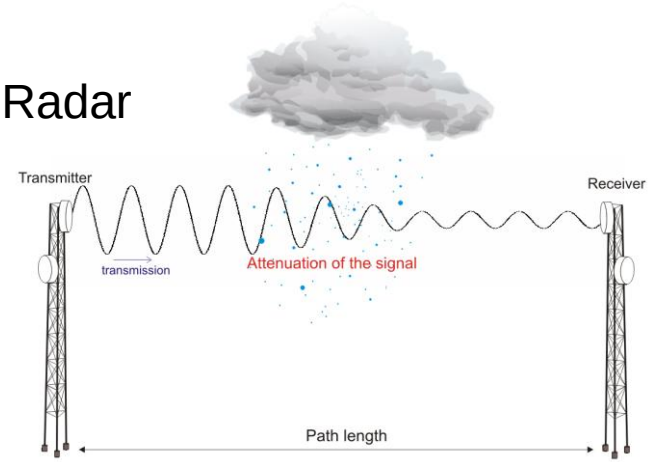

LTE, EPFL

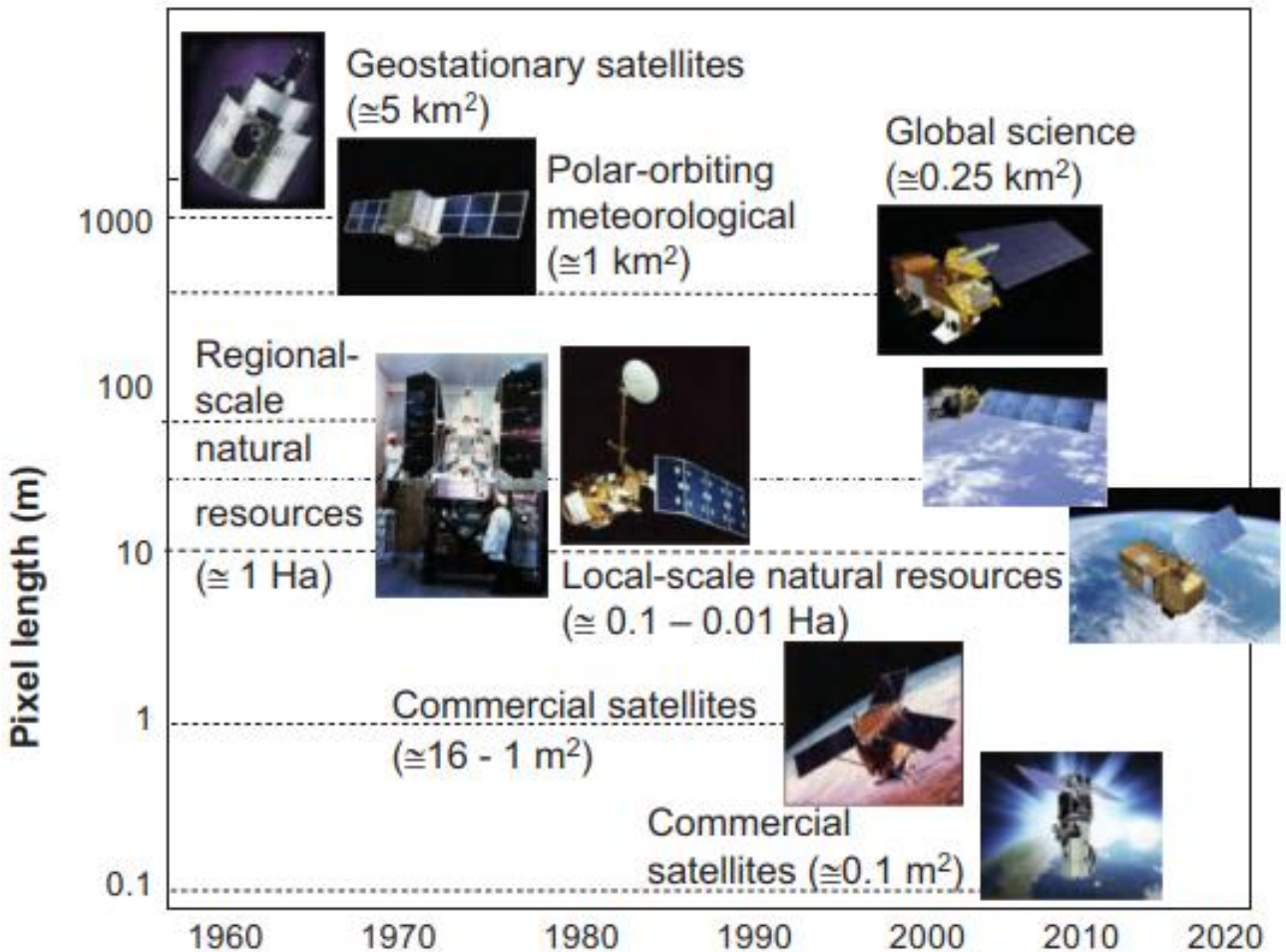

Chuvieco, 2020

Table 10.3 *List of selected acronyms.*

ACE-FTS	Atmospheric Chemistry Experiment Fourier Transform Spectrometer
AERONET	AErosol RObotic NET
AIRS	Atmospheric Infrared Sounder
AVHRR	Advanced Very High Resolution Radiometer
CALIOP	Cloud-Aerosol LIdar with Orthogonal Polarization
CALIPSO	Cloud-Aerosol Lidar and Infrared Pathfinder Satellite Observation
ERS-2	European Remote-Sensing Satellite-2
GEMS	Geostationary Environment Monitoring Spectrometer
GLAS	Geoscience Laser Altimeter System
GOES	Geostationary Operational Environmental Satellites
GOME	Global Ozone Monitoring Experiment
GOSAT	Greenhouse gases Observing SATellite
IASI	Infrared Atmospheric Sounding Interferometer
ICESat	Ice, Cloud and land Elevation Satellite
IMG	Interferometric Monitor for Greenhouse Gases
IRS	Infrared Sounder
MAPS	Mapping of Atmospheric Pollution from Space
MAX-DOAS	Multi Axis Differential Optical Absorption Spectroscopy
MERIS	MEdium Resolution Imaging Spectrometer
MIPAS	Michelson Interferometer for Passive Atmospheric Sounding
MISR	Multiangle Imaging SpectroRadiometer
MLS	Microwave Limb Sounder
MODIS	Moderate Resolution Imaging Spectroradiometer
MOPITT	Measurements Of Pollution In The Troposphere
OCO-2	Orbiting Carbon Observatory
OMI	Ozone Monitoring Instrument
OMPS	Ozone Mapping and Profiler Suite
OSIRIS	Optical Spectrograph and InfraRed Imager System
PARASOL	Polarization and Anisotropy of Reflectances for Atmospheric Sciences coupled with Observations from a Lidar
SCIAMACHY	SCanning Imaging Absorption SpectroMeter for Atmospheric CHartographY
TANSO	Thermal And Near infrared Sensor for carbon Observation
TEMPO	Tropospheric Emissions: Monitoring of Pollution
TES	Tropospheric Emission Spectrometer
TOMS	Total Ozone Mapping Spectrometer
TROPOMI	TROPOspheric Monitoring Instrument

Table 10.1 *Instruments used for nadir satellite remote sensing of tropospheric trace gases and aerosols.*

Instrument	Platform	Measurement period	Typical nadir resolution (km)	Equator crossing time[a]	Revisit time (days)[b]
GOME	ERS-2	1995–2011	320 × 40	10:30 d	3
MOPITT	Terra	2000–	22 × 22	10:30 d	3.5
MISR	Terra	2000–	18 × 18[c]	10:30 d	7
MODIS	Terra Aqua	2000–2002–	1 × 1[c]	10:30 d 1:30 a	2
AIRS	Aqua	2002–	14 × 14	1:30 a	1
SCIAMACHY	Envisat	2002–2012	60 × 30	10:00 d	6
OMI	Aura	2004–	24 × 13	1:45 a	1
TES	Aura	2004–	8 × 5	1:45 a	n/a
PARASOL	PARASOL	2004–	18 × 16	1:30 a	1
CALIOP	CALIPSO	2006–	40 × 40	1:30 a	n/a
GOME-2	MetOp	2006–	80 × 40	9:30 d	1
IASI	MetOp	2006–	12 × 12	9:30 d	0.5
TANSO-FTS	GOSAT	2009–	10 × 10	1:00 a	3
OMPS	NPP	2011–	50 × 50	1:30 a	1
VIIRS	NPP	2011–	10 × 10	1:30 a	1
OCO-2	OCO-2	2014–	1 × 2	1:30 a	16
TROPOMI	Sentinel-5 Precursor	2017–	7 × 7	1:30 a	1

[a]Crossing time occurs both a.m. and p.m. Descending daylit orbits are indicated by 'd' and ascending daylit orbits by 'a'.
[b]Value given for clear-sky conditions. Clouds impede the retrieval.
[c]Radiances for MISR, MODIS, and VIIRS are acquired at between 205 m and 1.1 km, depending on the channel. Resolutions reported here are for the finest aerosol products.

Chance and Martin, 2017

(Note this was from 2017 and some have since been retired.)

Borthomieu, 2014

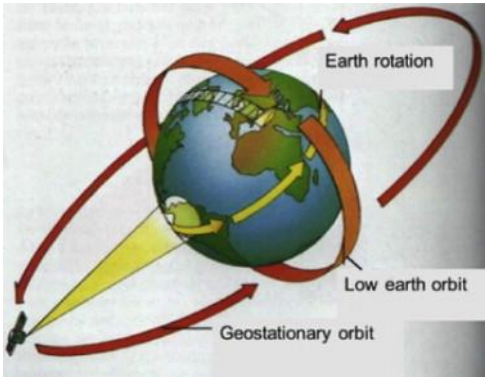

Geostationary: TEMPO, MAIA, GEMS, Sentinel-4

Table 10.2 *Satellite remote sensing of major tropospheric trace gases and aerosols.*[a]

Instrument	Spectral range (μm)	NO_2	H_2CO	SO_2	CO	O_3	NH_3	CH_4	CO_2	τ_a
GOME	0.23–0.79	X	X	X		0.5–1.5				
MOPITT	4.7				0.5–2					
MISR	4[b], $\lambda = 0.45 - 0.87$									X
MODIS	36[b], $\lambda = 0.41 - 14.2$									X
AIRS	3.7–16			X	0.5–1.5			X	X	
SCIAMACHY	0.23–2.3	X	X	X	X	0.5–1.5		X	X	
OMI	0.27–0.50	X	X	X		0.5–1.5				X
TES	3.3–15.4				0.5–1.5	1–2	X	X	X	
PARASOL	9[b], $\lambda = 0.44 - 1.0$									X
CALIOP	0.53–1.06									>30
GOME-2	0.24–0.79	X	X	X		0.5–1.5		X	X	
IASI	3.6–15.5				0.5–1.5	1–2	X			
TANSO-FTS	4[b], $\lambda = 0.76 - 14.3$							X	X	
OMPS	0.3–0.38	X	X	X		X				
VIIRS	22[b], $\lambda = 0.41 - 11.5$									X
OCO-2	3[b], $\lambda = 0.76 - 2.1$								X	
TROPOMI	0.27–2.4	X	X	X	X	0.5–1.5		X		X

[a] The number of independent degrees of freedom for signal in the troposphere is given for each instrument. An X indicates a tropospheric column.
[b] Number of discrete wavelength bands.

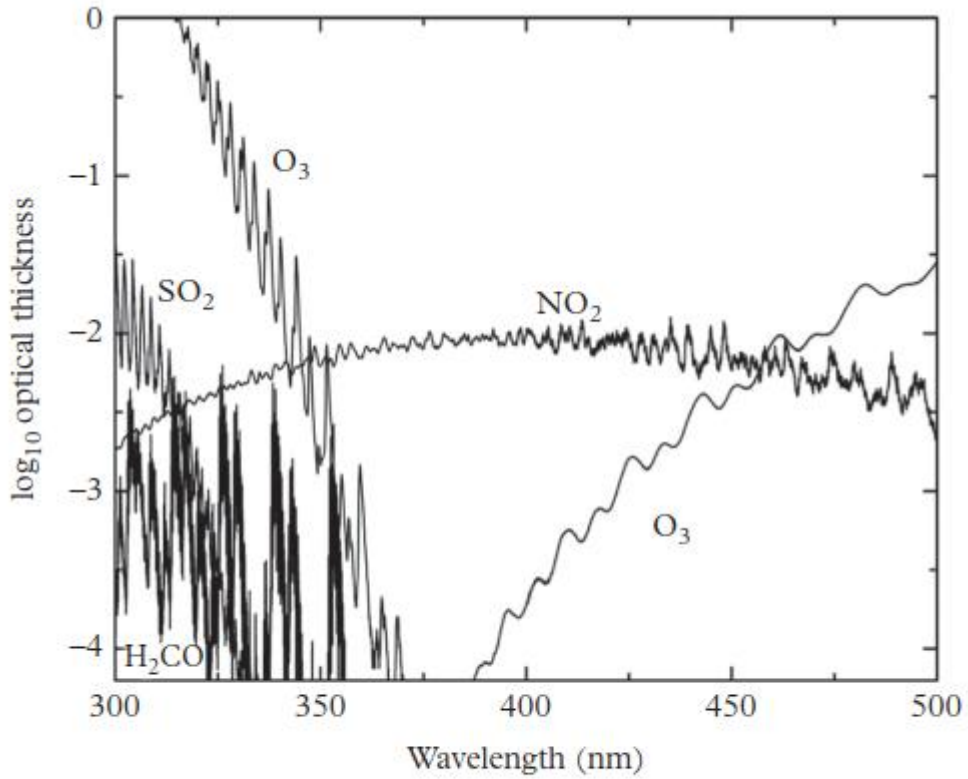

Figure 10.11 *Absorption optical depths for major air quality gases in the ultraviolet and visible.*

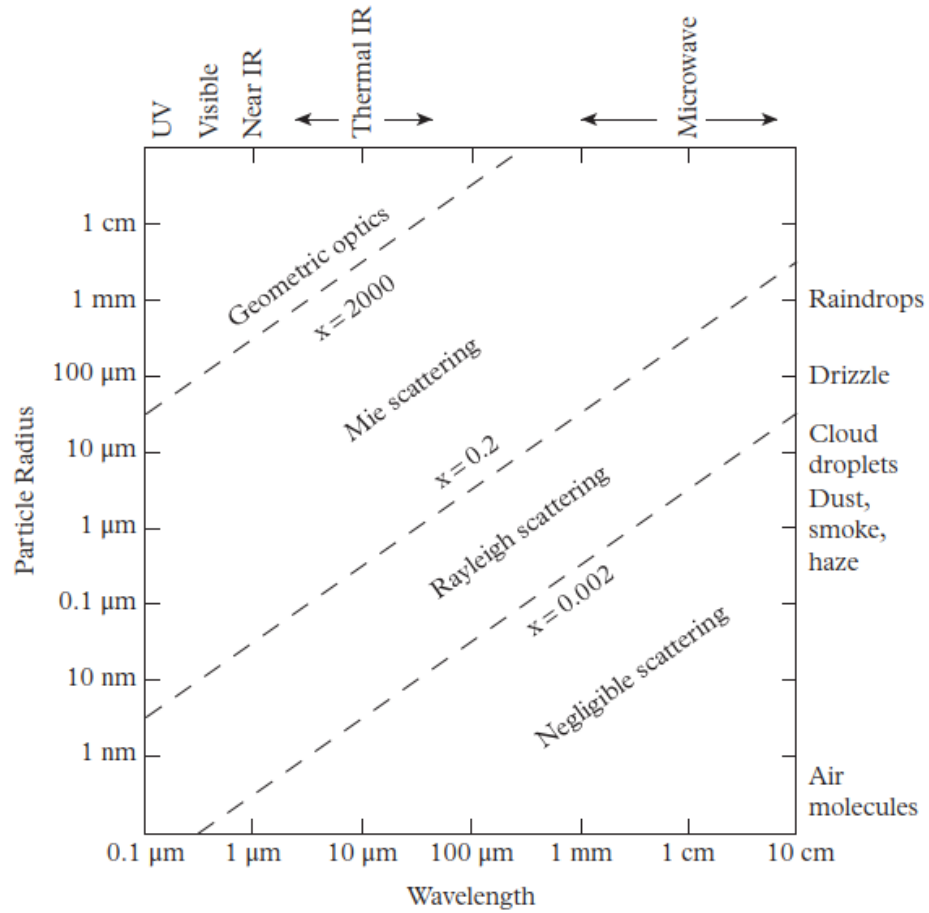

Figure 7.1 *Relationships among scattering particle size, radiation wavelength, and scattering behavior for atmospheric particles.*

Adapted from Atmospheric Science: An Introductory Survey, *J.M. Wallace and P.V. Hobbs, 1977, and* A First Course in Atmospheric Radiation, *G.W. Petty, 2006.*

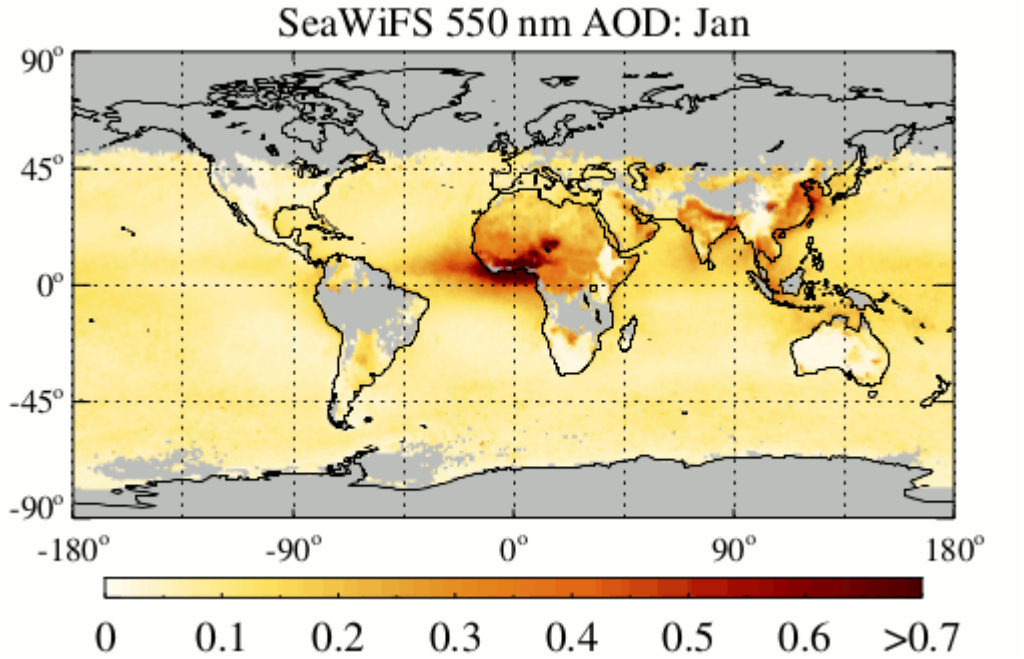

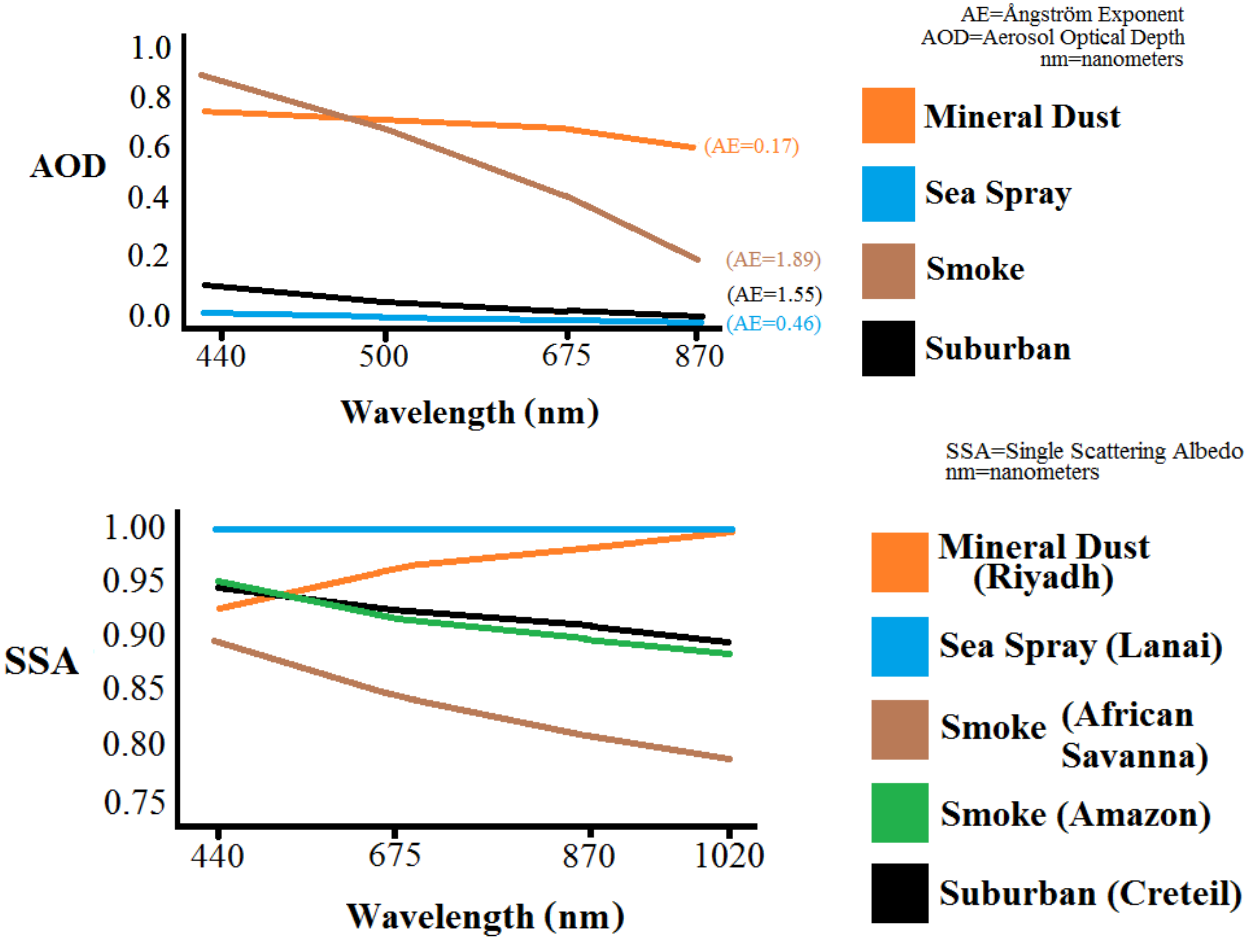

https://earth.gsfc.nasa.gov/climate/data/deep-blue/science

Wildfires in North America affecting air quality in the Arctic

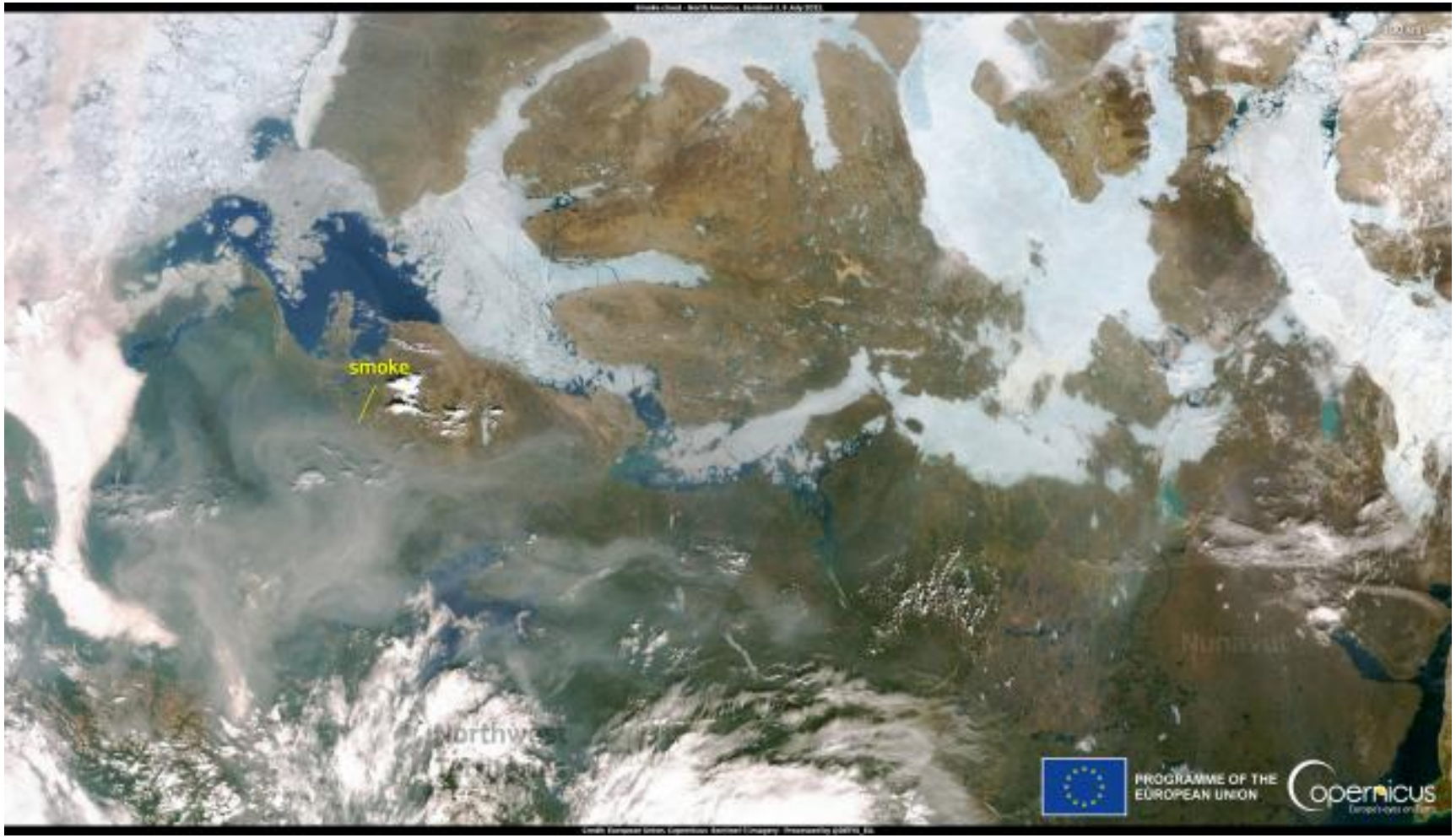

On 9 July 2022, one of the Copernicus Sentinel-3 satellites acquired this image, showing the smoke cloud generated by the wildfires engulfing the skies of the Northwestern Territories and Nunavut in Canada.

https://www.copernicus.eu/

Slides courtesy of Arindam Roy

Ship Emissions from Space

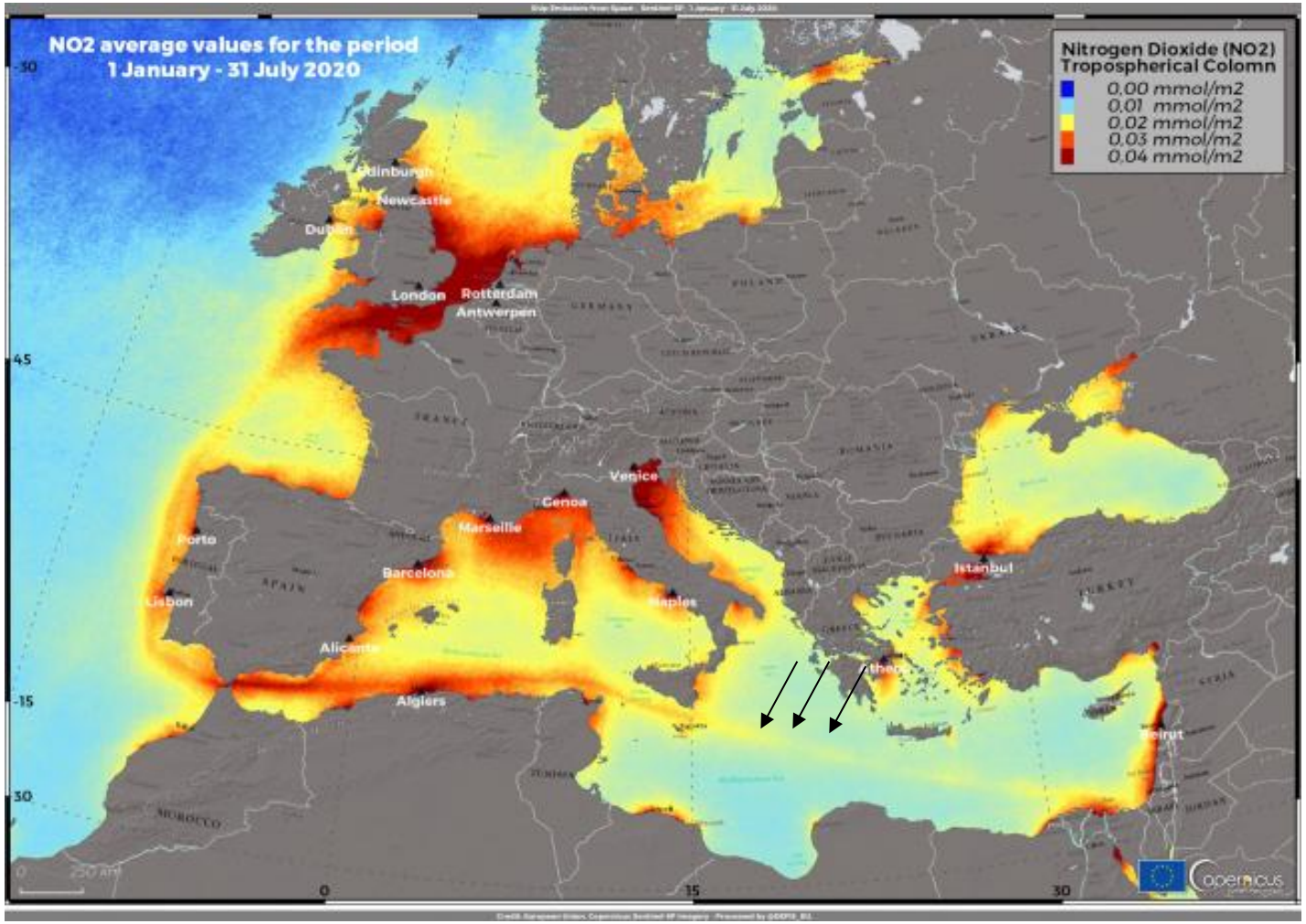

This image shows the average value of Tropospheric Nitrogen Dioxide (NO2) detected between January and July 2020 by the Copernicus Sentinel-5P Satellite for the open water areas of the European Region (Mediterranean Sea, Atlantic Ocean, etc).

https://www.copernicus.eu/

Fog in Northern India

The skies of Northern India are currently engulfed in a thick layer of fog, making for low visibility conditions and causing major disruptions to travel. The dense fog, visible in this image taken by the Copernicus Sentinel-3 satellite, has resulted in flight delays and cancellations at airports in the region, as well as delays for trains.

https://www.copernicus.eu/

Saharan Dust Event

In early April 2023, multiple plumes of Saharan dust were observed originating from Africa. On 4 April, Copernicus Sentinel-3 captured an image of a large plume stretching hundreds of kilometers from the coast of Libya to Türkiye.

https://www.copernicus.eu/

Fire in Europe

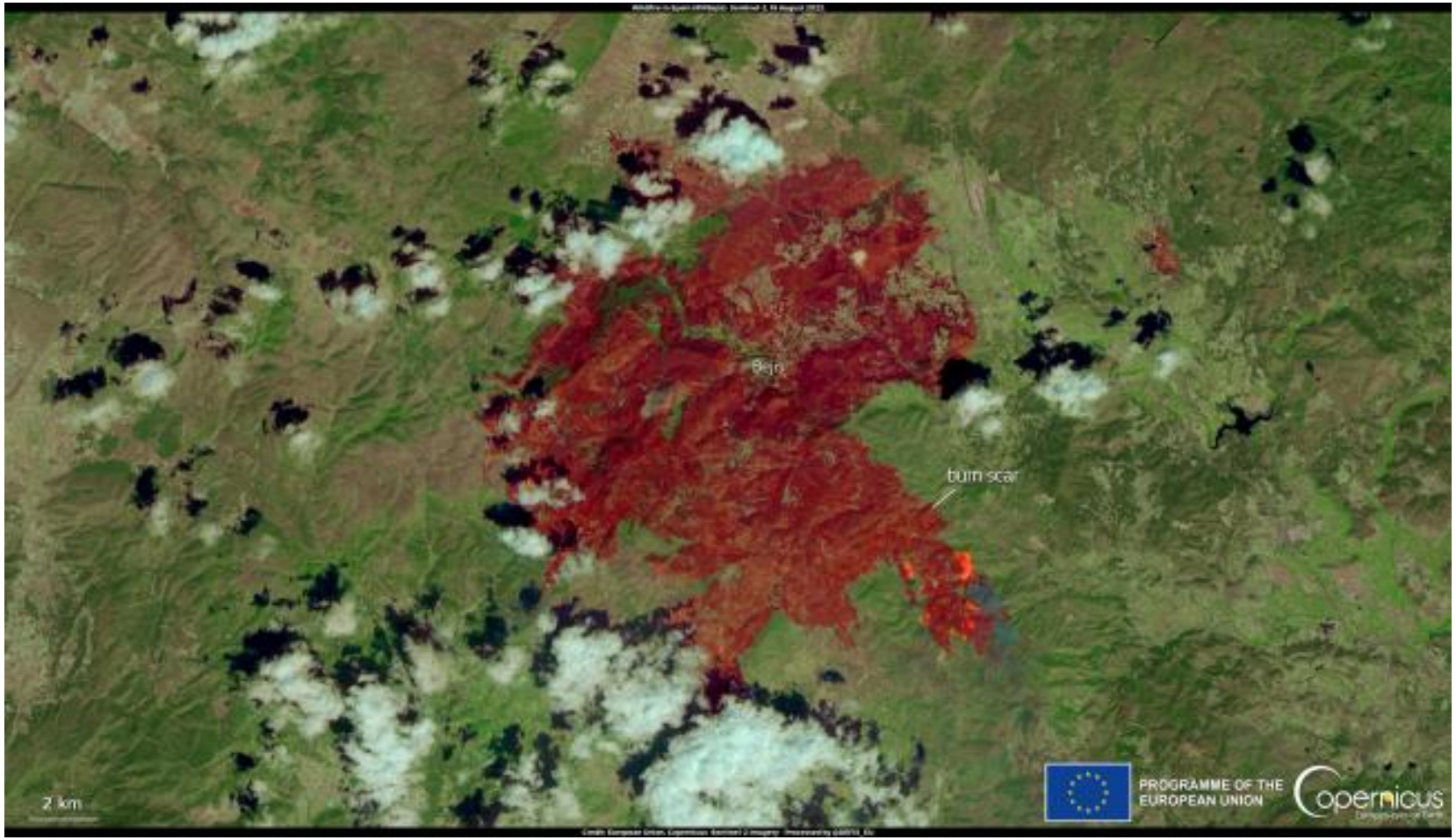

As shown in this image acquired by one of the Copernicus Sentinel-2 satellites on 18 August, a new disastrous fire is ongoing near Bejis, in the Valencian Autonomous Community. According to data from the European Forest Fire Information System (EFFIS), one of the modules of the Copernicus Emergency Management Service (CEMS), in 2022 more than 662,000 hectares have burnt in EU countries.

https://www.copernicus.eu/

Complementary monitoring strategies

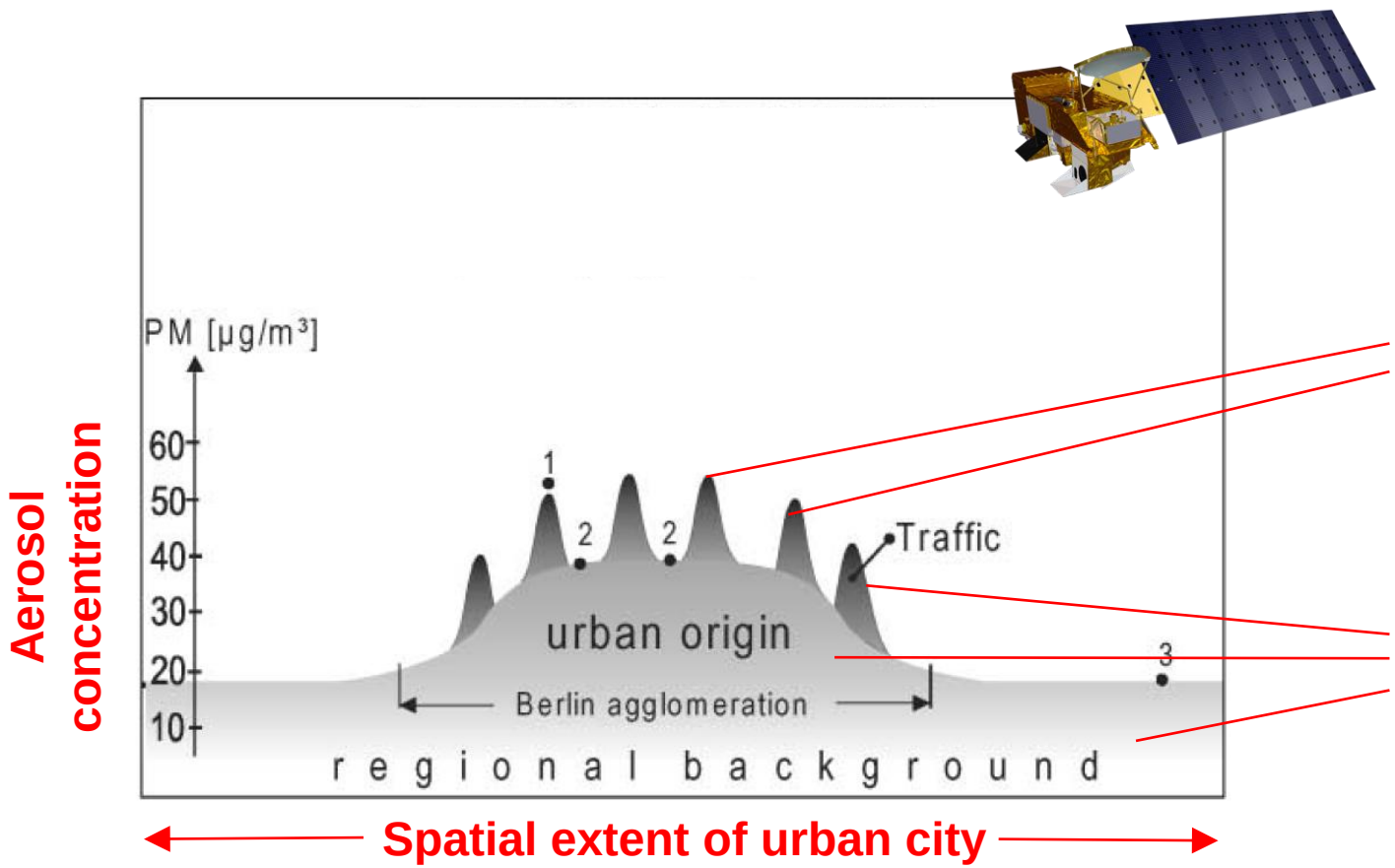

Satellite observation
(*intermittent, clear-sky coverage)*

Low-cost sensors
(*high spatial coverage, low data quality)*

Reference monitors
(*high data quality,*
*"chemical fingerprint" of sources***)**

Figure from Lenschow et al., *Atmos. Environ.*, 2001

References

- Bohren and Huffman, *Absorption and Scattering of Light by Small Particles*, John Wiley & Sons, 1983
- Chance and Martin, *Spectroscopy and Radiative Transfer of Planetary Atmospheres*, Oxford University Press, 2017
- Chuvieco, *Fundamentals of Satellite Remote Sensing*, CRC Press, 2020
- Efremenko and Kokhanovsky, *Foundations of Atmospheric Remote Sensing*, Springer, 2021
- Hapke, *Theory of Reflectance and Emittance Spectroscopy*, 2nd ed., Cambridge University Press, 2012
- Hecht, *Optics*, 5th ed., Pearson Education Limited, 2017
- Petty, *A First Course in Atmospheric Radiation*, 2nd ed., Sundog Publishing, 2006
- Seager, *Exoplanet Atmospheres: Physical Processes*, Princeton University Press, 2010.
- Seinfeld and Pandis, *Atmospheric Chemistry and Physics*, 2nd ed., John Wiley & Sons, 2016